Text-Video Retrieval with Global-Local Semantic Consistent Learning

Haonan Zhang, Pengpeng Zeng, Lianli Gao, Jingkuan Song, Yihang Duan, Xinyu Lyu, Heng Tao Shen, *Fellow, IEEE*

***Abstract*—Adapting large-scale image-text pre-training models, *e.g.,* CLIP, to the video domain represents the current state-of-the-art for text-video retrieval. The primary approaches involve transferring text-video pairs to a common embedding space and leveraging cross-modal interactions on specific entities for semantic alignment. Though effective, these paradigms entail prohibitive computational costs, leading to inefficient retrieval. To address this, we propose a simple yet effective method, Global-Local Semantic Consistent Learning (GLSCL), which capitalizes on latent shared semantics across modalities for text-video retrieval. Specifically, we introduce a parameter-free global interaction module to explore coarse-grained alignment. Then, we devise a shared local interaction module that employs several learnable queries to capture latent semantic concepts for learning fine-grained alignment. Furthermore, an Inter-Consistency Loss (ICL) is devised to accomplish the concept alignment between the visual query and corresponding textual query, and an Intra-Diversity Loss (IDL) is developed to repulse the distribution within visual (textual) queries to generate more discriminative concepts. Extensive experiments on five widely used benchmarks (*i.e.*, MSR-VTT, MSVD, DiDeMo, LSMDC, and ActivityNet) substantiate the superior effectiveness and efficiency of the proposed method. Remarkably, our method achieves comparable performance with SOTA as well as being nearly 220 times faster in terms of computational cost. Code is available at: https://github.com/zchoi/GLSCL.**

***Index Terms*—Text-Video Retrieval, Vision-and-Language Pre-training, CLIP model, Consistent Learning.**

I. Introduction

With the tremendous explosion of videos uploaded daily to sharing platforms, *e.g.,* TikTok, YouTube, and Netflix, searching for videos of interest with the text has become part of our daily life, necessitating an urgent need for effective text-video retrieval techniques [1]–[4]. Due to the huge cost of annotating large-scale text-video datasets, an emerging trend to solve this task is to transfer large-scale image-text pre-trained models [5], [6] with their powerful representation and generalization capabilities to the video domain [1], [7]. One of the representative models, CLIP [6] employs a dual-branch structure to learn cross-modal alignment trained on an extensive corpus of web-collected image-text pairs, making it naturally suitable for the text-video retrieval task [8], [9]. As a pioneering work, CLIP4Clip [8] successfully extends the above strategy by directly projecting text-video pairs into the same embedding space to perform global alignment.

Haonan Zhang (zchoiowal@gmail.com), Pengpeng Zeng, Lianli Gao, Jingkuan Song, Yihang Duan, Xinyu Lyu, Heng Tao Shen are Future Media Center and School of Computer Science and Engineering, University of Electronic Science and Technology of China.

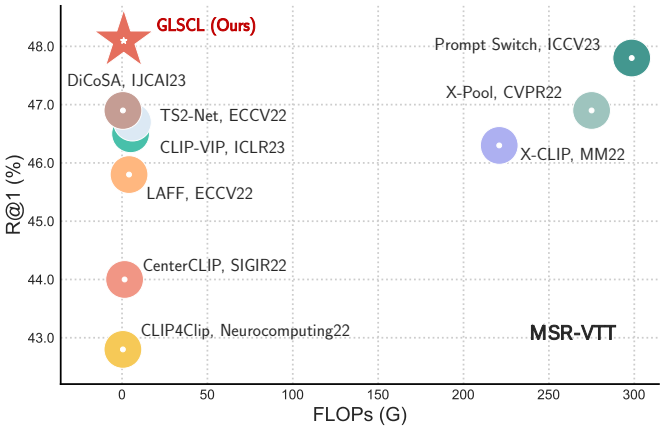

Fig. 1: **Performance comparison of the retrieval results (R@1) and computational costs (FLOPs) for text-to-video retrieval models, including existing state-of-the-art methods and our GLSCL.** For a fair comparison, we perform all results trained on the MSR-VTT dataset and all models adopt the CLIP-ViT-B/32 backbone. The white dots highlight the R@1 score of the blobs.

However, simply pooling all frames or all words as a whole representation may result in detailed information loss, affecting the retrieval performance [9]. Generally, a sentence is made up of words with varying properties and expresses local information about a video. Therefore, a feasible solution is to investigate detailed semantic alignments through fine-grained interactions [10], [11]. For instance, existing methods introduce a heavy cross-modal fusion module that concentrates on specific entities within the text (*e.g.,* words and phrases) and video (*e.g.,* patches and regions) modalities [10], [12] or design a parametric text-condition pooling to attend to the most semantically similar frames [11]. Although these methods have achieved remarkable performance gains, they encounter prohibitive computational costs, leading to inefficient retrieval for real applications, as shown in Fig. 1. Formally, given a text query set N_t, and a candidate video set N_v, where their average length and duration are N_w words and N_f frames, respectively. When performing more fine-grained interactions, the computational complexity is $\mathcal{O}(N_t N_v N_f N_w)$ (*e.g.,* X-CLIP) or $\mathcal{O}(N_t N_v N_f)$ (*e.g.,* X-Pool). As N_w and N_f become larger, the complexity increases dramatically. For CLIP4Clip, its complexity is $\mathcal{O}(N_t N_v)$, while its performance is inferior to X-Pool and X-CLIP. Thus, how to effectively and efficiently investigate cross-modal interactions for text-video retrieval remains to be explored.

To this end, we propose a **G**lobal-**L**ocal **S**emantic

Consistent **L**earning (GLSCL) for text-video retrieval task. The main idea behind our method is based on the observation that humans are swiftly adapting to summarizing information and then reasoning about it. To achieve this, we aim to uncover the latent shared semantics that exist across different modalities in a lightweight manner. Specifically, we first introduce a global interaction module (GIM) to facilitate a coarse-grained alignment at the sentence-video level, effectively mapping broad semantics across the text and video modalities. Notably, GIM is a parameter-free approach, requiring no additional parameters. Next, building upon the capabilities of the GIM module, we further devise a local interaction module (LIM) to handle the finer nuances of semantic alignment, thereby achieving a more precise and detailed understanding of the interactions between text and video content. To accomplish this, LIM utilizes a set of N_q learnable queries, each aimed at summarizing and capturing distinct and latent semantic concepts that emerge across text-video pairs. Moreover, to ensure a robust learning among these learnable queries, we introduce two specialized objective functions, *i.e.*, an inter-consistency loss (ICL) and an intra-diversity loss (IDL). In detail, the inter-consistency loss is proposed to assist the model in maintaining coherent semantics between the corresponding text-video queries. Conversely, the intra-diversity loss is developed to encourage a diversification within the text-video queries, accordingly fostering a rich semantic exploration and meanwhile mitigating the concept overlapping issue.

Effectiveness and Efficiency Analysis. Experimentally, Fig. 1 shows the quantitative performance comparison of the retrieval results (R@1) and computational costs (FLOPs) on the MSR-VTT dataset. Notably, our GLSCL achieves the best trade-off between the above two metrics as located in the upper left corner of the figure. For computational complexity, our method calculates the similarity scores at both coarse and fine-grained levels simultaneously. Unlike existing fine-grained approaches, LIM associates N_q latent semantics among cross-modality by the dot product operation. Particularly, it is worth noting that N_q is relatively small compared to N_f and N_w. Therefore, the final complexity of the proposed method is $\mathcal{O}(N_t N_v (1+N_q))$, which is significantly efficient than X-CLIP's $\mathcal{O}(N_t N_v N_f N_w)$ and X-Pool's $\mathcal{O}(N_t N_v N_f)$.

To summarize, our contributions are three-fold:

- We present a simple yet effective method, namely Global-Local Semantic Consistent Learning (GLSCL), which devises a parameter-free global interaction module (GIM) and a shared local interaction module (LIM) to explore both coarse and fine-grained alignments in a lightweight way.
- We present two novel learning objectives, *i.e.*, inter-consistency loss (ICL) and intra-diversity loss (IDL), to improve the model's matching accuracy. These unique loss functions focus on cultivating diverse and fostering coherent concept representations within and across semantic queries.
- Extensive experiments conducted on five commonly used datasets demonstrate that our GLSCL achieves the best trade-off between performance and computational complexity compared to the state-of-the-art methods.

II. Related Work

A. Vision-Language Pre-training

Vision-language pre-training aims to understand and process the relationship between image and text modalities. Benefiting from the achievements of self-supervised learning in uni-modal tasks, there is a growing interest in exploiting pre-training learning for cross-modal tasks, *e.g.,* vision-and-language [13]–[15]. Recently, the contrastive image-text pre-training [6], [14], [16] on large-scale web data has achieved great success for significant performance when transferring to various downstream tasks, such as VQA and image captioning. Specifically, as one of the striking pre-trained models, CLIP [6] has revealed powerful zero-shot ability [17] and domain generalization [18] that learns from tremendous image-text pairs with a contrastive loss. For video counterparts, large-scale video-text pre-training [19]–[21] has been shown promising results on video-language understanding. For instance, CLIPBERT [20] proposes an end-to-end framework for video-and-language tasks based on the pre-trained CLIP and BERT models, showcasing great performance and generalization abilities. Frozen in Time [21] takes advantage of both large-scale image and video captioning datasets and thus introduces a dual encoder model for text-video retrieval task. Nonetheless, pre-training typically requires dense and high-quality visual text datasets, with greater overhead for labeling large-scale video-text data compared to image-text data [22], [23]. To alleviate this burden, efforts like CLIP4Clip [8] and Prompt Switch [9] are made to adapt the image-text pretraining models to the video domain, showcasing their strong representation and excellent performance. Thus, this paper employs this scheme for the text-video retrieval task.

B. Text-Video Retrieval

Text-video retrieval is a challenging task that involves ranking videos based on their semantic relevance to a text query, and *vice versa*. Previous studies [10], [24], [25] focus on developing fusion strategies to align pre-extracted text and video features, such as W2VV [26] and HGR [10]. Recently, large-scale pre-trained image-text models such as CLIP [27] have shown exceptional performance and generalization across a wide range of image-text downstream tasks including image classification and visual recognition. Several works [9], [11] explore the powerful image-text pre-trained model to the video domain and achieve state-of-the-art performance. For instance, CLIP4Clip [8] models temporal contexts on top of the CLIP to better align video clips and text query, which shows a great performance improvement. X-Pool [11] uses a cross-modal attention mechanism to weighted aggregate video frames conditioned on text semantics for a better representation of the video. HBI [28] treats video and text as game players in game theory, and leverages hierarchical Banzhaf interactions to aggregate video frame tokens and text word tokens into higher-level representations, which represents the complex relationships between video and text in greater detail. Albeit these promising advances, existing methods still suffer from the huge computational cost, thereby leading to a dilemma in achieving a balanced trade-off between effectiveness and

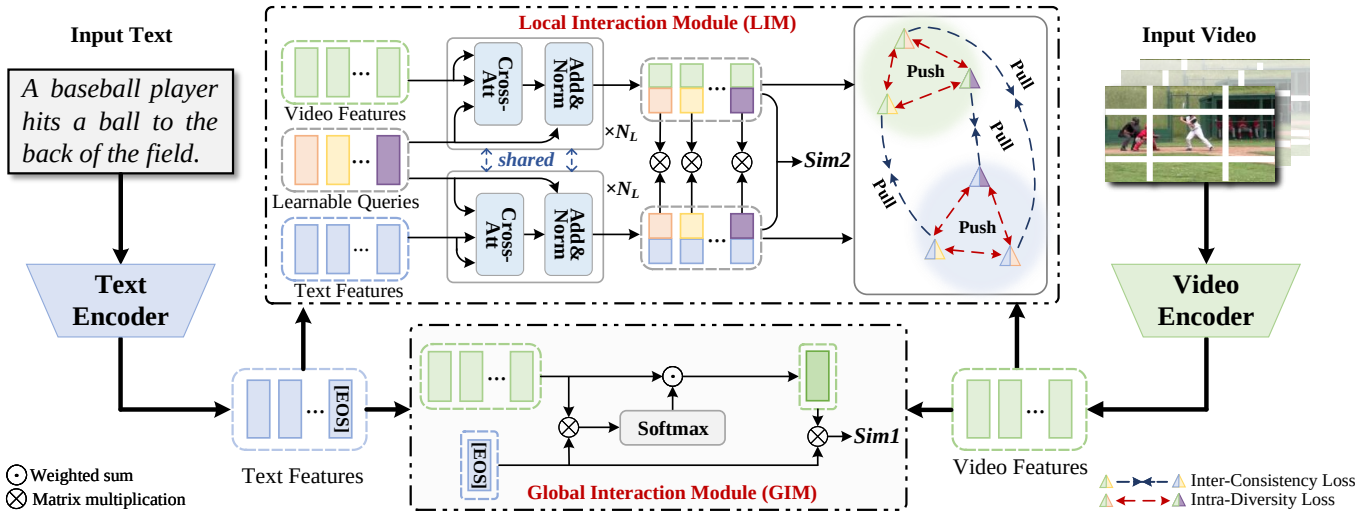

Fig. 2: **Overview of the proposed GLSCL for text-video retrieval.** It comprises two main components: (1) Global Interaction Module (GIM) captures coarse-level semantic information among text and video data without involving trainable parameters, and (2) Local Interaction Module (LIM) achieves fine-grained alignment within a shared latent semantic space via several lightweight queries. Furthermore, we introduce an inter-consistency loss and an intra-diversity loss to guarantee consistency and diversity of the shared semantics across and within modalities, respectively.

efficiency for real applications. To this end, we propose an effective and computationally feasible method for text-video retrieval from both coarse- and fine-grained aspects to tackle these limitations.

III. Method

In this section, we present our Global-Local Semantic Consistent Learning (GLSCL) for text-video retrieval. To be specific, we begin with a brief overview including the task formulation of text-video retrieval and the basic pipeline of the proposed method in Sec. III-A. Then, we present the explanation about two designed modules, *i.e.*, global interaction module (GIM) and local interaction module (LIM) in Sec. III-B and III-C. Consequently, we provide a detailed description about the devised consistent learning strategy, containing two novel objective functions, *i.e.*, inter-consistency loss (ICL) and intra-diversity loss (IDL) in Sec. III-D. At last, we introduce the training details for text-video retrieval task in Sec. III-E. The overall architecture is depicted in Fig. 2.

A. Overview

Task Formulation. Let $\mathcal{D} \in \{\mathcal{T}, \mathcal{V}\}$ be a text-video collection, where $\mathcal{T}$ is a set of sentences and $\mathcal{V}$ is a set of videos. The objective of text-to-video retrieval is to rank all videos in $v \in \mathcal{V}$ given the text query t based on a similarity score $\mathcal{S}(t, v)$, and *vice versa* for video-to-text retrieval.

Formally, to extract text features, given an input text $t = \{t_n\}_{n=1}^{N_w}$ with N_w words, we first leverage the text encoder $\mathcal{F}_t$ of pre-trained CLIP [6] to extract word features $\boldsymbol{t}' = \mathcal{F}_t(t) \in \mathbb{R}^{N_w \times D}$. Then we take the `[EOS]` embedding as the sentence feature $\tilde{\boldsymbol{t}} \in \mathbb{R}^D$, where D indicates the feature dimension.

For the video features, we begin by dividing a video sample $v = \{f_k\}_{k=1}^{N_f}$ with N_f frames into fix-sized disjoint patches prepended with a `[CLS]` token. Then, the pre-processed video frames are sent into the video encoder $\mathcal{F}_v$ of the pre-trained CLIP model to extract frame features. After that, combing `[CLS]` token and frame features and taking them as input, a temporal transformer (TT) [8] is adopted to acquire temporal perception across frames sequence. The above operations are formalized as follows:

$$\begin{aligned} \hat{\boldsymbol{f}}_k &= \mathcal{F}_v(f_k) \in \mathbb{R}^{M \times D}, \\ [\boldsymbol{f}'_1, ..., \boldsymbol{f}'_k, ..., \boldsymbol{f}'_{N_f}] &= TT([\hat{\boldsymbol{f}}^0_1, ..., \hat{\boldsymbol{f}}^0_k, ..., \hat{\boldsymbol{f}}^0_{N_f}]) \in \mathbb{R}^{N_f \times D}, \end{aligned} \tag{1}$$

where $\hat{\boldsymbol{f}}_k$ stands for the k-th frame feature from CLIP's encoder and $\hat{\boldsymbol{f}}^0_k$ is marked as the `[CLS]` embedding of k-th frame. Here, we denote $\boldsymbol{v}' = [\boldsymbol{f}'_1, ..., \boldsymbol{f}'_k, ..., \boldsymbol{f}'_{N_f}]$ as the frame features output from temporal transformer, and M stands for the number of patches plus a `[CLS]` token.

To further enhance the visual cues, especially those associated with the text semantics, we adopt the proposed global interaction module (GIM) to obtain text-guided video feature $\tilde{\boldsymbol{v}}$:

$$\tilde{\boldsymbol{v}} = GIM(\boldsymbol{v}', \tilde{\boldsymbol{t}}) \in \mathbb{R}^D. \tag{2}$$

Moreover, to effectively capture more fine-grained semantic relationships, we introduce a local interaction module (LIM). Different from previous methods that involve heavy fusion modules to interact with specific entities in both text and video modalities, LIM achieves fine-grained alignment by acquiring latent semantics at word-level and frame-level via a set of lightweight learnable queries $\boldsymbol{u} = \{\boldsymbol{u}_i\}_{i=1}^{N_q}$:

$$\begin{aligned} \boldsymbol{c}^v &= LIM(\boldsymbol{u}, \boldsymbol{v}') \in \mathbb{R}^{N_q \times D}, \\ \boldsymbol{c}^t &= LIM(\boldsymbol{u}, \boldsymbol{t}') \in \mathbb{R}^{N_q \times D}, \end{aligned} \tag{3}$$

where N_q denotes the number of learnable queries. Next, we will elaborate on the details of the proposed GIM and LIM in the subsequent subsections.

B. Global Interaction Module

The proposed global interaction module (GIM) stands out as a coarse-grained interaction mechanism that captures global semantics at the sentence-video level. It calculates the weights between text and frame features and aggregates the frame feature to obtain the text-guided video feature:

$$\begin{aligned} \alpha_k &= \frac{\exp(\tilde{\boldsymbol{t}}^\top \boldsymbol{f}'_k/\tau)}{\sum_{j=1}^{N_f}\exp(\tilde{\boldsymbol{t}}^\top \boldsymbol{f}'_j/\tau)}, \\ \tilde{\boldsymbol{v}} &= \sum_{k=1}^{N_f}\alpha_k \boldsymbol{f}'_k, \end{aligned} \tag{4}$$

where α_k denotes the text-conditioned weight for the k-th frame feature, and τ indicates a scaling factor. It is noted that GIM achieves a balance between effectiveness and efficiency without any learnable parameters involved.

C. Local Interaction Module

Recent fine-grained approaches [9], [11] rely on elaborated fusion modules to enable interaction between specific entities in text and video modalities. However, these methods are often computationally expensive in real-world retrieval applications. To this, we propose a local interaction module (LIM) to address the aforementioned limitations by capturing the fine-grained semantic clues in a shared learning manner.

As described in III-A, we first initialize several learnable queries $\boldsymbol{u} = \{\boldsymbol{u}_i\}_{i=1}^{N_q}$ to encourage conceptual semantic sharing among text and video data. To that end, we employ N_L transformer blocks to acquire the most relevant semantics by interacting queries with the frame features $\boldsymbol{v}'$ and the word features $\boldsymbol{t}'$ respectively. Given the video side as an example, the operation on the l-th transformer block can be formulated as:

$$\begin{aligned} \boldsymbol{u}_l^v &= \texttt{Concat}^{(l-1)}\left(\mathbf{h}_0, \mathbf{h}_1, ..., \mathbf{h}_H\right)\boldsymbol{W}^O, \\ \mathbf{h}_z &= \texttt{Attention}^{(l-1)}\left(\boldsymbol{Q}\boldsymbol{W}_z^Q, \boldsymbol{K}\boldsymbol{W}_z^K, \boldsymbol{V}\boldsymbol{W}_z^V\right), \end{aligned} \tag{5}$$

where $\boldsymbol{u}_l^v \in \mathbb{R}^{N_q \times D}$ denotes the encoded queries obtained from l-th block, here $\boldsymbol{K} = \boldsymbol{V} = \boldsymbol{v}'$ and $\boldsymbol{Q} = \boldsymbol{u}_{l-1}^v$. Moreover, $\boldsymbol{W}_z^Q$, $\boldsymbol{W}_z^K$, $\boldsymbol{W}_z^V$, $\boldsymbol{W}^O$ are learnable weight matrices, H is the number of heads, and $\mathbf{h}_z$ is the output of z-th head. Note that the initial learnable queries are treated as the input of the transformer blocks $\boldsymbol{u}_0^v = \boldsymbol{u}$, and we take the output of the last block as the summarized visual concepts $\boldsymbol{c}^v = \boldsymbol{u}_{N_L}^v$. Similarly, we can obtain the summarized textual concepts $\boldsymbol{c}^t$ with the same operation.

Here, to maintain the model size, we share the parameters of learnable queries and transformer blocks among visual and textual encoders. Also, this approach allows the model to implicitly learn the semantic interactions between the two types of input, leading to improved matching accuracy of the model. The detailed experimental results are presented in Sec. IV-C.

D. Inter-consistency and Intra-diversity Learning

a) Inter-Consistency Loss: Although we adopt shared learnable queries among vision and text encoders, there may still exist *'semantic-asymmetric'* issue between generated visual and textual concepts. To address this problem, we propose an inter-consistency loss (ICL) to facilitate better semantic alignment during model training. Firstly, we consider the Euclidean distance constraint to encourage the i-th textual concept $\boldsymbol{c}_i^t$ close to its corresponding visual concept $\boldsymbol{c}_i^v$:

$$\mathcal{D}^i = \|\boldsymbol{c}_i^t - \boldsymbol{c}_i^v\|_2^2. \tag{6}$$

Then, in order to avoid overfitting between two types of concepts, we devise a semantic regularization by constraining the positive video-text concepts in a suitable margin as follows:

$$\gamma = \sum_{i=1}^{N_q}(\lambda - (\boldsymbol{c}_i^t)^\top \boldsymbol{c}_i^v)^2, \tag{7}$$

where λ is a slack factor that controls the minimum semantic distance between each positive text-video concept ($\boldsymbol{c}_i^t$, $\boldsymbol{c}_i^t$). Finally, the inter-consistency loss is defined as:

$$\mathcal{L}_{\texttt{ICL}} = \sum_{i=1}^{N_q}\mathcal{D}^i + \gamma. \tag{8}$$

b) Intra-Diversity Loss: To alleviate the overlapping clustering of matched video-text concepts learned by ICL, we further propose to promote the discrimination within the visual and textual concepts, effectively dealing with the multi-context collapse problem [29], [30]. To achieve this goal, we introduce an intra-diversity loss (IDL). Specifically, taking visual concepts as an example, we first calculate the relevance using a cosine similarity function:

$$o_{i,j}^v = \texttt{COS}(\boldsymbol{c}_i^v, \boldsymbol{c}_j^v) = (\boldsymbol{c}_i^v)^\top \boldsymbol{c}_j^v, \tag{9}$$

where $o_{i,j}^v$ represents the semantic distance between i-th video concept $\boldsymbol{c}_i^v$ and j-th video concept $\boldsymbol{c}_j^v$.

Then, we enlarge these distance between concepts in a common semantic space:

$$\mathcal{L}_{\texttt{IDL}}^v = \frac{1}{N_q}\sum_{i=1, i\neq j}^{N_q}[\max(0, \Delta + o_{i,j}^v - o_{i,i}^v)], \tag{10}$$

where Δ is a slack factor. Similarly, we adopt the same constraint on the text side and obtain the final intra-diversity learning loss:

$$\mathcal{L}_{\texttt{IDL}} = \frac{1}{2}(\mathcal{L}_{\texttt{IDL}}^v + \mathcal{L}_{\texttt{IDL}}^t). \tag{11}$$

E. Training Details

a) Similarity Score: During the model training and inference, we calculate the similarity matrix from two aspects: i) coarse-grained similarity score $\mathcal{S}_{\texttt{C}}$, which measures the global semantic alignment at sentence-video level, and ii) fine-grained similarity score $\mathcal{S}_{\texttt{F}}$, which explores fine-grained concept matching to achieve local semantic alignment. Then we add the matching score and concept score to obtain the

TABLE I: **Performance comparison with the state-of-the-art on the MSR-VTT dataset.** * denotes that the methods utilize QB-NORM as the post-processing operation to achieve better performance. - means that these results are unavailable in the original paper. Since these methods all adopt CLIP as the backbone, we only test the FLOPs of the similarity calculation head.

Methods	Text ⇒ Video					Video ⇒ Text					FLOPs
	R@1↑	R@5↑	R@10↑	MdR↓	MnR↓	R@1↑	R@5↑	R@10↑	MdR↓	MnR↓	
CLIP-ViT-B/32											
CLIP4Clip*[Neurocomputing'22]*	44.5	71.4	81.6	2.0	15.3	42.7	70.9	80.6	2.0	11.6	0.5G
CenterCLIP*[SIGIR'22]*	44.2	71.6	82.1	2.0	15.1	42.8	71.7	82.2	2.0	10.9	1.5G
X-CLIP*[MM'22]*	46.1	73.0	83.1	2.0	13.2	46.8	73.3	84.0	2.0	9.1	220.9G
TS2-Net*[ECCV'22]*	47.0	74.5	83.8	2.0	13.0	45.3	74.1	83.7	2.0	9.2	6.1G
X-Pool*[CVPR'22]*	46.9	72.8	82.2	2.0	14.3	44.4	73.3	84.0	2.0	9.0	275.0G
CLIP-VIP*[ICLR'23]*	46.5	72.1	82.5	-	-	-	-	-	-	-	0.5G
DiCoSA*[IJCAI'23]*	46.7	75.0	82.9	2.0	13.0	44.1	73.5	82.7	2.0	9.8	0.51G
DiCoSA**[IJCAI'23]*	47.5	74.7	83.8	2.0	13.2	46.7	75.2	84.3	2.0	8.9	0.51G
Prompt Switch*[ICCV'23]*	47.8	73.9	82.2	-	14.1	46.0	74.3	84.8	-	8.5	298.5G
GLSCL (ours)	48.1	73.9	82.3	2.0	13.8	47.1	73.0	83.2	2.0	10.3	1.0G
GLSCL* (ours)	50.0	73.7	82.8	1.5	14.2	49.4	74.5	83.9	2.0	9.6	1.0G
CLIP-ViT-B/16											
CLIP4Clip*[Neurocomputing'22]*	45.6	71.2	80.9	2.0	15.2	43.2	72.5	80.7	2.0	10.9	0.5G
CenterCLIP*[SIGIR'22]*	48.4	73.8	82.0	2.0	13.8	47.7	75.0	83.3	2.0	10.2	1.5G
X-CLIP*[MM'22]*	49.3	75.8	84.8	2.0	12.2	48.9	76.8	84.5	2.0	8.1	220.9G
GLSCL (ours)	49.5	75.1	83.9	2.0	12.6	48.9	76.3	85.8	2.0	8.4	1.0G
GLSCL* (ours)	50.5	75.2	83.8	1.0	12.8	49.2	76.1	86.2	2.0	8.5	1.0G

final retrieval score. The detailed calculation is formulated as follows:

$$\begin{aligned} \mathcal{S}_{\text{C}}(t,v) &= \frac{\tilde{\boldsymbol{t}}\cdot\tilde{\boldsymbol{v}}}{\|\tilde{\boldsymbol{t}}\|\|\tilde{\boldsymbol{v}}\|}, \\ \mathcal{S}_{\text{F}}(\boldsymbol{c}^t,\boldsymbol{c}^v) &= \frac{1}{N_q}\sum_{i=1}^{N_q}\frac{\boldsymbol{c}_i^t\cdot\boldsymbol{c}_i^v}{\|\boldsymbol{c}_i^t\|\|\boldsymbol{c}_i^v\|}, \\ \mathcal{S} &= \mathcal{S}_{\text{C}}+\xi\mathcal{S}_{\text{F}}, \end{aligned} \tag{12}$$

where ξ is a weighting factor.

b) Loss Functions: Following previous works [8], [11], [31], we first calculate the contrastive loss as the primary objective:

$$\begin{aligned} \mathcal{L}_{\text{CL}} = \frac{1}{2}[&\frac{1}{B}\sum_{b=1}^{B}\log\frac{e^{s(t_b,v_b)/\pi}}{\sum_{r=1}^{B}e^{s(t_b,v_r)/\pi}}+ \\ &\frac{1}{B}\sum_{b=1}^{B}\log\frac{e^{s(t_b,v_b)/\pi}}{\sum_{r=1}^{B}e^{s(t_r,v_b)/\pi}}], \end{aligned} \tag{13}$$

where B means the mini-batch size, π is a learnable temperature factor, and $\mathcal{S}(t_b,v_r)$ refers to the similarity matrix between text t_b and video v_r.

Then, we combine the two proposed losses above (Sec. III-D), *i.e.*, *inter-consistency loss* $\mathcal{L}_{\text{ICL}}$ and an *intra-diversity loss* $\mathcal{L}_{\text{IDL}}$, with $\mathcal{L}_{\text{CL}}$ as the final loss function to optimize our model:

$$\mathcal{L}_{\text{total}} = \mathcal{L}_{\text{CL}}+\alpha\mathcal{L}_{\text{ICL}}+\beta\mathcal{L}_{\text{IDL}}, \tag{14}$$

where α and β are the trade-off hyper-parameters.

IV. EXPERIMENTS

A. Experiment Setup

a) Datasets: We report experimental results on five widely used benchmarks for text-video retrieval, including: (1) **MSR-VTT** [32] contains 10,000 video clips, each annotated with 20 sentences. Following [33], we utilize 9,000 clips for training and the remaining clips for testing. (2) **MSVD** [34] crawls 1,970 videos from YouTube, with approximately 40 descriptive sentences per video, where 1,200, 100, and 670 videos are used for training, validation, and testing, respectively. (3) **DiDeMo** [35] collects 10K Flikr videos annotated with 40K captions. This dataset is evaluated using a video-paragraph retrieval manner provided in [8]. (4) **LSMDC** [36] consists of 118,081 short video clips, with each video clip typically paired with a single caption. For a fair comparison, we adopt the split provided by [37] that uses 109,673, 7,408, and 1,000 videos for training, validation, and testing, respectively. (5) **ActivityNet** [38] includes 20,000 videos with 200 different types of human activities. We adopt the same setting in [33] to validate our model.

b) Evaluation Metrics: Following the existing approaches [8], [33], we employ common retrieval metrics to evaluate the performance of the model, including R@K (Recall at Rank K, higher is better ↑), Median Rank (MdR, lower is better ↓), and Mean Rank (MnR, lower is better ↓). Here, K is set to 1, 5, and 10.

c) Implementation Details: Following [11], [33], we utilize the CLIP checkpoints to initialize the text encoder and video encoder. The temporal transformer comprises 4 transformer blocks, initialized by CLIP's text encoder. For MSR-VTT, MSVD, and LSMDC datasets, we uniformly sample $N_f = 12$ frames per video and set the max length of the caption as $N_w = 32$. For ActivityNet and DiDeMo datasets, each video is sampled over $N_f = 64$ frames, and the max sentence length is set to $N_w = 64$ for better learning. Note that each frame is resized to 224×224 and divided into $M = 49$ patches for all datasets. The feature dimension D is 512 and the number of attention heads H is 8. We set the number of learnable queries to $N_q = 8$ for all datasets, and $N_L = 3$ transformer blocks are applied in LIM. Unless

TABLE II: **Performance comparison with state-of-the-art on the MSVD, DiDeMo, LSMDC, and ActivityNet datasets.** We report both text-to-video and video-to-text results, and all models employ only CLIP-ViT-B/32 without considering post-processing operations. † indicates the reproduced results using public code provided by the corresponding paper for a fair comparison.

Methods	MSVD				DiDeMo				LSMDC				ActivityNet			
	R@1↑	R@5↑	R@10↑	MnR↓	R@1↑	R@5↑	R@10↑	MnR↓	R@1↑	R@5↑	R@10↑	MnR↓	R@1↑	R@5↑	R@10↑	MnR↓
Text-to-Video Retrieval																
CLIP4Clip*[Neurocomputing'22]*	45.2	75.5	84.3	10.3	42.8	68.5	79.2	18.9	22.6	41.0	49.1	61.0	40.5	72.4	83.6	7.5
CenterCLIP*[SIGIR'22]*	47.3	76.9	86.0	9.7	-	-	-	-	21.4	39.7	49.4	55.9	43.9	74.6	85.8	6.7
X-CLIP*[MM'22]*	47.1	77.8	-	9.5	45.2	74.0	-	14.6	23.3	43.0	-	56.0	44.3	74.1	-	7.9
TS2-Net*[ECCV'22]*	-	-	-	-	41.8	71.6	82.0	14.8	23.4	42.3	50.9	56.9	41.0	73.6	84.5	8.4
X-Pool*[CVPR'22]*	47.2	77.4	86.0	9.3	-	-	-	-	25.2	43.7	53.5	53.2	-	-	-	-
CLIP-VIP*[ICLR'23]*	-	-	-	-	40.6	70.4	79.3	-	-	-	-	-	-	-	-	-
DiCoSA†*[IJCAI'23]*	43.4	73.4	82.9	11.6	41.8	73.1	82.1	13.3	22.8	41.5	50.5	57.9	37.8	68.6	81.8	8.1
Prompt Switch*[ICCV'23]*	47.1	76.9	86.1	9.5	-	-	-	-	23.1	41.7	50.5	56.8	-	-	-	-
GLSCL (ours)	47.5	76.3	86.1	9.8	46.7	75.0	82.9	13.0	23.4	42.4	49.8	56.2	41.4	72.1	83.9	7.5
Video-to-Text Retrieval																
CLIP4Clip*[Neurocomputing'22]*	62.0	87.3	92.6	4.3	41.4	68.2	79.1	12.4	20.8	39.0	48.6	54.2	41.4	73.7	85.3	6.7
CenterCLIP*[SIGIR'22]*	63.5	86.4	92.6	3.8	-	-	-	-	19.5	39.9	48.0	50.1	44.5	75.7	86.2	6.5
X-CLIP*[MM'22]*	60.9	87.8	-	4.7	43.1	72.2	-	10.9	22.5	42.2	-	50.7	43.9	73.9	-	7.6
TS2-Net*[ECCV'22]*	-	-	-	-	-	-	-	-	-	-	-	-	-	-	-	-
X-Pool*[CVPR'22]*	66.4	90.0	94.2	3.3	-	-	-	-	22.7	42.6	51.2	47.4	-	-	-	-
CLIP-VIP*[ICLR'23]*	-	-	-	-	-	-	-	-	-	-	-	-	-	-	-	-
DiCoSA†*[IJCAI'23]*	61.7	88.1	89.3	5.5	44.0	73.8	82.2	9.7	20.3	39.8	49.8	51.6	36.5	69.3	82.2	7.7
Prompt Switch*[ICCV'23]*	68.5	91.8	95.6	2.8	-	-	-	-	22.0	40.8	50.3	51.0	-	-	-	-
GLSCL (ours)	69.1	91.5	94.8	3.2	45.9	74.5	83.1	9.5	22.2	41.4	50.0	50.3	40.6	71.8	84.1	7.1

TABLE III: **Ablation study of shared strategy for learnable query (LQ) and transformer block (TB).** ♠ and ♣ denote unshared and shared learning strategies, respectively. '#Param.' means the number of trainable parameters.

LQ	TB	Text ⇒Video					#Param.
		R@1↑	R@5↑	R@10↑	MdR↓	MnR↓	
♠	♠	46.3	73.2	81.7	2.0	13.7	112.5M
♣	♠	46.6	73.5	83.2	2.0	13.7	110.4M
♠	♣	47.6	73.5	82.5	2.0	12.9	101.3M
♣	♣	48.1	73.9	82.3	2.0	13.8	99.2M

TABLE IV: **Ablation study of learning objective in GLSCL.** $\mathcal{L}_{\text{CL}}$, $\mathcal{L}_{\text{ICL}}$ and $\mathcal{L}_{\text{IDL}}$ represent contrastive loss, inter-consistency loss, and intra-diversity loss. $\mathcal{S}_{\text{C}}$ and $\mathcal{S}_{\text{F}}$ mean coarse-grained similarity score and fine-grained similarity score, respectively.

$\mathcal{L}_{\text{CL}}$		$\mathcal{L}_{\text{ICL}}$	$\mathcal{L}_{\text{IDL}}$	Text ⇒ Video				
$\mathcal{S}_{\text{C}}$	$\mathcal{S}_{\text{F}}$			R@1↑	R@5↑	R@10↑	MdR↓	MnR↓
✓	✗	✗	✗	45.2	71.7	81.5	2.0	14.7
✓	✓	✗	✗	46.4	73.4	81.8	2.0	14.0
✓	✓	✓	✗	47.8	73.2	82.6	2.0	13.9
✓	✓	✗	✓	47.1	73.4	82.4	2.0	13.8
✓	✓	✓	✓	48.1	73.9	82.3	2.0	13.8

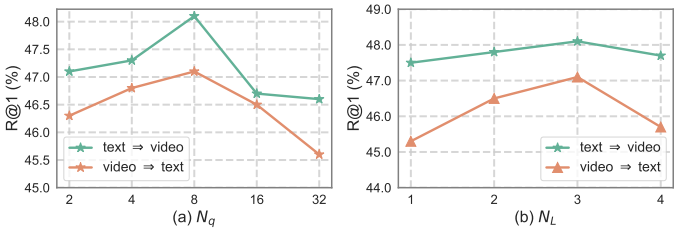

Fig. 3: **Ablation studies of the number of learnable queries N_q and transformer blocks N_L.**

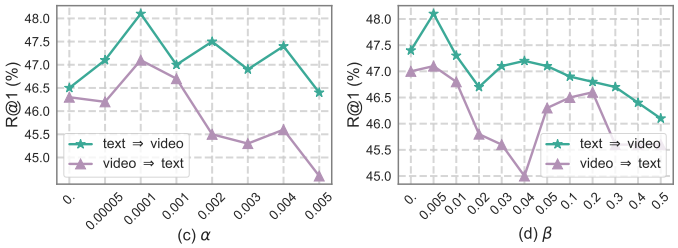

Fig. 4: **Ablation study of hyper-parameters α and β in Eq. 14.**

otherwise stated, we set the hyper-parameters $\alpha = 0.0001$, $\beta = 0.005$, $\xi = 0.5$, $\pi = 0.01$, and $\tau = 5$ as default. The two slack factors λ and Δ are set to 0.75 and 0.1, respectively. For model training, we utilize Adam [39] as the optimizer with a linear warmup and train the network in 5 epochs with 128 mini-batch sizes. The initial learning rate is set to $1e-7$ for text and video encoders and $1e-3$ for the other trainable modules.

B. Performance Comparisons

a) Compared methods: In this section, we compare our method GLSCL with state-of-the-art methods, including CLIP4Clip [8], CenterCLIP [40], X-CLIP [12], TS2-Net [41], X-Pool [11], CLIP-VIP [7], DiCoSA [33], and Prompt Switch [9]. Note that all methods utilize CLIP-ViT as the backbone.

b) Results on MSR-VTT dataset: The comparison results on the MSR-VTT dataset are presented in Tab. I, which illustrate retrieval performance as well as computational costs (FLOPs) on CLIP-ViT-B/32 and CLIP-ViT-B/16. Overall, our method achieves the best trade-off between performance and computational costs. In particular, building on CLIP-ViT-B/32 without QB-NORM [42], GLSCL outperforms all compared models, with the best results being R@1 = 48.1% for text-to-video retrieval and R@1 = 47.1% for video-to-text retrieval. Additionally, compared with the SOTA method, *i.e.*, Prompt Switch, our method has a lower computational cost, which is approximately 220 times reduced. Beyond that, at roughly the same computational cost, GLSCL yields 1.4% and 3.0% improvement than DiCoSA on R@1 for text-to-video and video-to-text retrieval, respectively. And our method with QB-NORM leads to a further performance improvement. After being equipped with a stronger visual backbone, *i.e.*, CLIP-ViT-B/16, our GLSCL achieves a further performance boost and

Fig. 5: **Visualization of the weight assignment.** Based on the attention weights derived from the third transformer block in LIM, a connection is established between the frame/word and the query that has the highest degree of association with it. For the sake of clarity, the assignments between some unimportant words and queries are omitted.

maintains admirable performance when compared with other methods. These results clearly demonstrate the effectiveness of our proposed method.

c) Results on other datasets: To demonstrate the robustness of our method, we further provide quantitative results on other datasets, including MSVD, DiDeMo, LSMDC, and ActivityNet. Tab. II showcases performance comparison for text-to-video retrieval and video-to-text retrieval results, and all models use only CLIP-ViT-B/32 without any post-processing operations. From the table, we observe that our GLSCL consistently improves the performance on MSVD and DiDeMo datasets and achieves comparable results on LSMDC and ActivityNet datasets. For instance, GLSCL surpasses the best counterpart method, *i.e.*, Prompt Switch, on both MSVD and ActivityNet datasets in R@1 (*e.g.,* 47.5% *v.s.* 47.1% and 23.4% *v.s.* 23.1 in $t2v$, 69.1% *v.s.* 68.5% and 22.2% *v.s.* 22.0 in $v2t$). For DiDeMo dataset, our method also achieves the best results in comparison with existing approaches. Besides, we also find some failure cases, *e.g.,* on the ActivityNet dataset, GLSCL fails to bring clear performance gains on both $t2v$ and $v2t$ splits. Possible reason is that ActivityNet involves more complex and long-term movie videos, the optimal hyperparamters for GLSCL on this dataset may be different, while we fix them (*e.g.,* the number of learnable queries) across all datasets and baselines. Due to the limited space, the computational costs for these methods are omitted in this table, while the approximate FLOPs are comparable to the values reported in Tab. I, indicating that our method is a more efficient way.

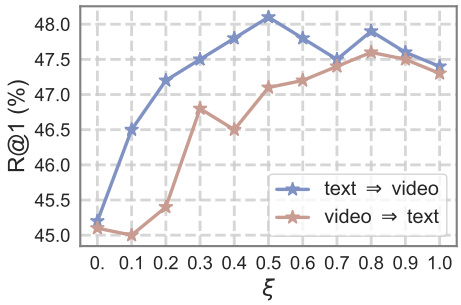

Fig. 6: **Ablation studies of the weighting factor ξ in Eq. 12.**

C. Ablation Study

To verify the impact of essential components of GLSCL, we conduct detailed ablation studies on the MSR-VTT dataset, where all experiment settings are built on the CLIP-ViT-B/32 backbone.

a) Effect of the shared strategy: In Tab. III, we study the impact of the shared strategy for learnable queries (LQ) and transformer blocks (TB). From the table, we notice that employing the shared strategy for LQ, TB, or both yields better R@1 results than the unshared strategy. The possible reason is that such a strategy implicitly facilitates the interaction between video and textual data, thus bridging the semantic gap between them. Moreover, there is an advantage to using a shared strategy to keep parameters smaller, which is also in line with our goal, *i.e.*, effectiveness and efficiency. Thus, we choose this strategy for the remaining experiments.

b) Effect of the learning objective: We attempt to investigate the influence of different learning objectives for

TABLE V: **Computational cost of text-video retrieval models.** Here, the inference time is for the entire test set. N_t, N_v, N_f, N_w, N_q indicate the number of text set, video set, frames, words, and queries respectively. For a fair comparison, all models adopt CLIP-ViT-B/32 backbone with 64 mini-batch sizes. Experiments are performed on MSR-VTT-1K-A with a 24GB NVIDIA RTX 4090 GPU.

Method	**R@1** ($t2v$)	**R@1** ($v2t$)	**Memory Demands**	**Inference Time**	**Time Complexity**
CLIP4Clip (base)	44.5	42.7	6360MB	35.016s	$\mathcal{O}(N_tN_v)$
CLIP-VIP	46.5	-	8626MB	37.920s	$\mathcal{O}(N_tN_v)$
DiCoSA	46.7	44.1	6726MB	**21.688s**	$\mathcal{O}(N_tN_v)$
CenterCLIP	44.2	42.8	6960MB	39.340s	$\mathcal{O}(N_tN_vN_f)$
TS2-Net	47.0	45.3	7148MB	36.929s	$\mathcal{O}(N_tN_vN_f)$
X-Pool	46.9	44.4	6584MB	59.736s	$\mathcal{O}(N_tN_vN_f)$
Prompt Switch	47.8	46.0	6877MB	68.589s	$\mathcal{O}(N_tN_vN_f)$
X-CLIP	46.1	46.8	6678MB	44.309s	$\mathcal{O}(N_tN_vN_fN_w)$
GLSCL (ours)	**48.1**	**47.1**	**6506MB**	36.622s	$\mathcal{O}(N_tN_v(1+N_q))$

GLSCL with five control groups: (i) baseline: $\mathcal{L}_{\texttt{CL}}$ only with $\mathcal{S}_{\texttt{C}}$; (ii) baseline with $\mathcal{S}_{\texttt{F}}$; (iii) adding $\mathcal{L}_{\texttt{ICL}}$ into (ii); (iv) adding $\mathcal{L}_{\texttt{IDL}}$ into (ii); and (v) full model that integrates all of the aforementioned learning objectives. The experimental results are shown in Tab. IV. Compared with baseline (i), incorporate $\mathcal{S}_{\texttt{F}}$ (ii) achieves better performance, demonstrating the shared semantic alignment is beneficial for text-video matching. Next, individually incorporating the proposed $\mathcal{L}_{\texttt{ICL}}$ (iii) and $\mathcal{L}_{\texttt{IDL}}$ (iv) into the model (ii) both brings a further performance enhancement. This reveals the advancement of the proposed losses, ensuring the consistency and diversity of concepts during the model training. Finally, combining all variants above (v) reaches the best performance.

c) Effect of number of learnable queries N_q: To assess how many learnable queries the model required to learn, we conduct experiments with different query numbers $N_q \in \{2, 4, 8, 16, 32\}$. The results are shown in Fig. 3 (a). Empirically, the larger the value of N_q, the more latent semantic information it will acquire and *vice versa*. However, our observation from this figure is that a continuous increase in the number of queries does not invariably result in a consistent improvement in performance. Notably, when $N_q = 8$, the model achieves the best result.

d) Effect of number of transformer blocks N_L: We adopt several transformer blocks as an information bottleneck upon learnable queries in the LIM module, to determine how many blocks are suitable for capturing latent semantics, we set the range of block number N_L from 1 to 4, as shown in Fig. 3 (b). Concretely, the performance of GLSCL gradually increases as the N_L grows from 1 to 3, after which continually enlarging N_L weakens the alignment ability and undermines the performance. In particular, GLSCL establishes the best performance when $N_L = 3$ on both two splits. Therefore, we empirically set the N_L to 3 in the remaining experiments.

e) Effect of hyper-parameters α and β: In Eq. 14, the hyper-parameters α and β respectively indicate the importance of $\mathcal{L}_{\texttt{ICL}}$ and $\mathcal{L}_{\texttt{IDL}}$ during the model optimization. Here, we evaluate the scale range of α and β from $[0, 0.005]$ and $[0, 0.5]$ as shown in Fig. 4 (a) and (b), respectively. From the table, the retrieval results both get improved with the increase of α and β, and peaked at $\alpha = 0.0001$ and $\beta = 0.005$ (*i.e.*, $t2v$/$v2t$: 48.1%/47.1% in R@1) before decreasing with larger α and β. Ultimately, we figure out the best value of α and β as 0.0001 and 0.005 for the final model.

f) Effect of hyper-parameter ξ: In Eq. 12, the hyper-parameter ξ indicates the importance of the fine-grained similarity score $\mathcal{S}_{\texttt{F}}$. To this end, we verify the impact of ξ by setting different values ranging from $[0, 1]$, as illustrated in Fig. 6. We find that the retrieval performance first improves before reaching the saturation point, *i.e.*, $\xi = 0.5$, and then begins to decline slightly. Thus, we empirically choose the best value for ξ as 0.5 in our final model.

g) Analysis for additional complexity costs: This paper seeks to examine effective and efficient methods for investigating cross-modal interactions for text-video retrieval. To this end, we report the detailed complexity costs of the existing methods and our GLSCL including memory demands, inference time, and time complexity as shown in Tab. V. Note that CLIP4Clip serves as the baseline method. The table reveals the following key observations: **i)** GLSCL obtains the best R@1 results (**48.1%/47.1%** on $t2v$/$v2t$) while exhibiting minimal memory growth compared to other methods. **ii)** In terms of inference time, GLSCL is slower than DiCoSA but still outperforms other methods, securing the second position. **iii)** Furthermore, we summarize the time complexity of existing methods (last column), which can be categorized into three groups: ① $\mathcal{O}(N_tN_v)$: global coarse-grained alignment, ② $\mathcal{O}(N_tN_vN_f)$: text-condition fine-grained alignment, and ③ $\mathcal{O}(N_tN_vN_fN_w)$: cross-modal fine-grained alignment. In contrast, our GLSCL captures the coarse and fine-grained alignments simultaneously: **(1)** $\mathcal{O}(N_tN_v)$: a simple yet effective global matching. **(2)** $\mathcal{O}(N_tN_vN_q)$: employing N_q queries to capture latent semantics among modality via dot product. Thus, the overall complexity of GLSCL is $\mathcal{O}(N_tN_v(1+N_q))$. Since N_q is relatively smaller than N_f and N_w, the complexity of GLSCL is comparable and much lower than ① and ②&③. The results further indicate the efficiency and flexibility of the proposed method for practical retrieval process.

D. Qualitative Analysis

The core of our proposed GLSCL is to capture latent semantics shared among text and video samples via a set of learnable queries for a fine-grained alignment. To ascertain whether the model has effectively acquired this capability, we showcase the assignment of attention weights for both word sequences and video frames on learnable queries in Fig. 5. As observed, the words and the frames with similar semantics have been successfully assigned to the same query. In particular, as shown in the top example, the word 'man' is most associated with query 2, and the video frames categorized under this query also encapsulate the related appearance characteristics. Furthermore, the term 'basket' exhibits the highest relevance with query 6, and the frames assigned to this query also effectively represent the 'basket-related' visual scenarios. In the bottom example, the words 'pirate' and 'man' are assigned to query 1, and the video frames belonging to query 1 also contain analogous semantic content. These examples illustrate that the proposed method can achieve a reliable fine-grained alignment via a shared semantic way.

To further qualitatively validate the effectiveness of the proposed method, we also provide text-to-video retrieval results

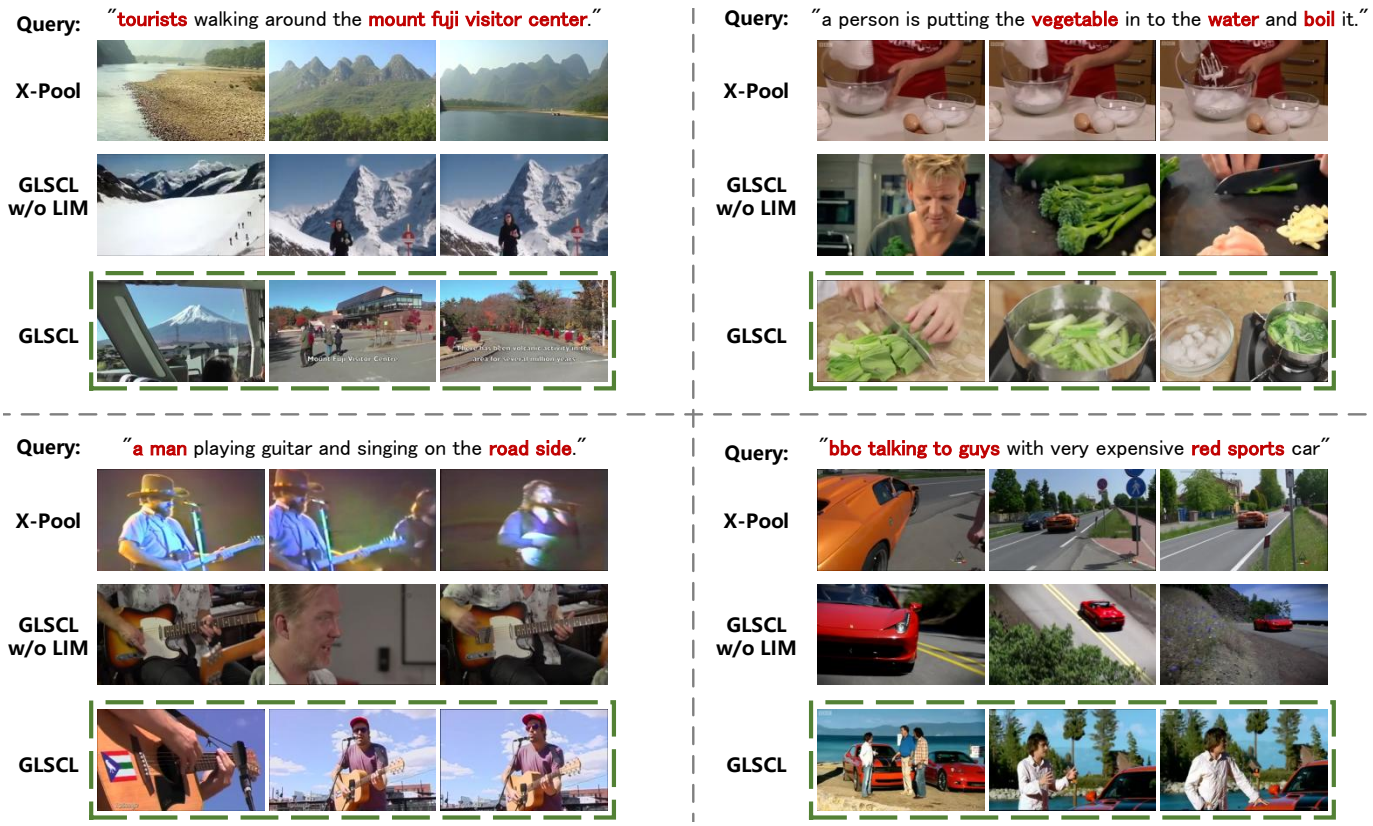

Fig. 7: **Qualitative analysis of text-to-video results, including X-Pool [11] and our methods (GLSCL w/o LIM and GLSCL). Given the text query, we provide the R@1 result of each method on the MSR-VTT dataset. Note that the correctly retrieved videos and related words are highlighted in `green` and `red` respectively.**

with three models, including X-Pool, GLSCL w/o LIM, and GLSCL, as shown in Fig. 7. In the top two examples, we observe that although X-Pool and GLSCL w/o LIM understand the concept of 'mount' and 'vegetable', they fail to ignore the detailed visual semantics, such as 'tourists', 'visitor center', 'water', and 'boil'. However, GLSCL successfully retrieves the correct videos from the gallery, showing the detailed semantic perception of LIM. The rest of the examples have similar properties. These results further demonstrate that our method can match the video with text query by capturing the visual contents from both coarse- and fine-grained semantic levels effectively.

V. Conclusion

This work proposes Global-Local Semantic Consistent Learning (GLSCL), a novel and simple method exploring how to effectively and efficiently investigate cross-modal interaction for text-video retrieval task. As a lightweight training framework, our GLSCL consistently facilitates the coarse-grained alignment through a global interaction module (GIM) and performs fine-grained alignment via a local interaction module (LIM). Notably, GIM acts as a parameter-free component to capture global semantic interaction between video-text modalities while LIM employs a semantic-shared learning strategy to acquire the co-occurred concepts among data pairs. Furthermore, to effectively capture invariant and diverse semantics across and within video-text modalities, we propose inter-consistency loss (ICL) and intra-diversity loss (IDL) to jointly enhance the matching performance of the model. Extensive experiments on five text-video retrieval benchmarks clearly confirm the effectiveness and efficiency of GLSCL, thereby establishing the best trade-off between performance and computational cost in comparison with state-of-the-art methods.

References

[1] S. Huang, B. Gong, Y. Pan, J. Jiang, Y. Lv, Y. Li, and D. Wang, "Vop: Text-video co-operative prompt tuning for cross-modal retrieval," in *CVPR*, 2023, pp. 6565–6574.

[2] J. Zhu, P. Zeng, L. Gao, G. Li, D. Liao, and J. Song, "Complementarity-aware space learning for video-text retrieval," *TCSVT*, 2023.

[3] M. Qi, J. Qin, Y. Yang, Y. Wang, and J. Luo, "Semantics-aware spatial-temporal binaries for cross-modal video retrieval," *TIP*, vol. 30, pp. 2989–3004, 2021.

[4] P. Wu, J. Liu, X. He, Y. Peng, P. Wang, and Y. Zhang, "Toward video anomaly retrieval from video anomaly detection: New benchmarks and model," *TIP*, vol. 33, pp. 2213–2225, 2024.

[5] R. Liu, J. Huang, G. Li, J. Feng, X. Wu, and T. H. Li, "Revisiting temporal modeling for clip-based image-to-video knowledge transferring," in *CVPR*, 2023, pp. 6555–6564.

[6] A. Radford, J. W. Kim, C. Hallacy, A. Ramesh, G. Goh, S. Agarwal, G. Sastry, A. Askell, P. Mishkin, J. Clark *et al.*, "Learning transferable visual models from natural language supervision," in *ICML*. PMLR, 2021, pp. 8748–8763.

[7] H. Xue, Y. Sun, B. Liu, J. Fu, R. Song, H. Li, and J. Luo, "Clip-vip: Adapting pre-trained image-text model to video-language representation alignment," in *ICLR*, 2023.

[8] H. Luo, L. Ji, M. Zhong, Y. Chen, W. Lei, N. Duan, and T. Li, "Clip4clip: An empirical study of clip for end to end video clip retrieval and captioning," *Neurocomputing*, vol. 508, pp. 293–304, 2022.

[9] C. Deng, Q. Chen, P. Qin, D. Chen, and Q. Wu, "Prompt switch: Efficient clip adaptation for text-video retrieval," in *ICCV*, 2023, pp. 15 648–15 658.

[10] S. Chen, Y. Zhao, Q. Jin, and Q. Wu, "Fine-grained video-text retrieval with hierarchical graph reasoning," in *CVPR*, 2020, pp. 10 638–10 647.

[11] S. K. Gorti, N. Vouitsis, J. Ma, K. Golestan, M. Volkovs, A. Garg, and G. Yu, "X-pool: Cross-modal language-video attention for text-video retrieval," in *CVPR*, 2022, pp. 5006–5015.

[12] Y. Ma, G. Xu, X. Sun, M. Yan, J. Zhang, and R. Ji, "X-clip: End-to-end multi-grained contrastive learning for video-text retrieval," in *ACM MM*, 2022, pp. 638–647.

[13] Y.-C. Chen, L. Li, L. Yu, A. El Kholy, F. Ahmed, Z. Gan, Y. Cheng, and J. Liu, "Uniter: Universal image-text representation learning," in *ECCV*. Springer, 2020, pp. 104–120.

[14] L. Yuan, D. Chen, Y.-L. Chen, N. Codella, X. Dai, J. Gao, H. Hu, X. Huang, B. Li, C. Li *et al.*, "Florence: A new foundation model for computer vision," *arXiv preprint arXiv:2111.11432*, 2021.

[15] J. Li, D. Li, S. Savarese, and S. Hoi, "Blip-2: Bootstrapping language-image pre-training with frozen image encoders and large language models," in *ICLR*, 2023.

[16] H. Tan and M. Bansal, "Lxmert: Learning cross-modality encoder representations from transformers," *arXiv preprint arXiv:1908.07490*, 2019.

[17] Z. Guo, R. Zhang, L. Qiu, X. Ma, X. Miao, X. He, and B. Cui, "Calip: Zero-shot enhancement of clip with parameter-free attention," in *AAAI*, vol. 37, no. 1, 2023, pp. 746–754.

[18] M. Singha, H. Pal, A. Jha, and B. Banerjee, "Ad-clip: Adapting domains in prompt space using clip," in *ICCV*, 2023, pp. 4355–4364.

[19] W. Shen, J. Song, X. Zhu, G. Li, and H. T. Shen, "End-to-end pre-training with hierarchical matching and momentum contrast for text-video retrieval," *TIP*, 2023.

[20] J. Lei, L. Li, L. Zhou, Z. Gan, T. L. Berg, M. Bansal, and J. Liu, "Less is more: Clipbert for video-and-language learning via sparse sampling," in *CVPR*, 2021, pp. 7331–7341.

[21] M. Bain, A. Nagrani, G. Varol, and A. Zisserman, "Frozen in time: A joint video and image encoder for end-to-end retrieval," in *ICCV*, 2021, pp. 1728–1738.

[22] A. Miech, D. Zhukov, J.-B. Alayrac, M. Tapaswi, I. Laptev, and J. Sivic, "Howto100m: Learning a text-video embedding by watching hundred million narrated video clips," in *ICCV*, 2019, pp. 2630–2640.

[23] T. Wang, Y. Ge, F. Zheng, R. Cheng, Y. Shan, X. Qie, and P. Luo, "Accelerating vision-language pretraining with free language modeling," in *CVPR*, 2023, pp. 23 161–23 170.

[24] Z. Wang, X. Xu, J. Wei, N. Xie, Y. Yang, and H. T. Shen, "Semantics disentangling for cross-modal retrieval," *TIP*, vol. 33, pp. 2226–2237, 2024.

[25] N. C. Mithun, J. Li, F. Metze, and A. K. Roy-Chowdhury, "Learning joint embedding with multimodal cues for cross-modal video-text retrieval," in *ICMR*, 2018, pp. 19–27.

[26] J. Dong, X. Li, and C. G. Snoek, "Predicting visual features from text for image and video caption retrieval," *TMM*, vol. 20, no. 12, pp. 3377–3388, 2018.

[27] K. Xia, L. Wang, S. Zhou, N. Zheng, and W. Tang, "Learning to refactor action and co-occurrence features for temporal action localization," in *CVPR*, 2022, pp. 13 884–13 893.

[28] P. Jin, J. Huang, P. Xiong, S. Tian, C. Liu, X. Ji, L. Yuan, and J. Chen, "Video-text as game players: Hierarchical banzhaf interaction for cross-modal representation learning," in *CVPR*, 2023, pp. 2472–2482.

[29] A. Sablayrolles, M. Douze, C. Schmid, and H. Jégou, "Spreading vectors for similarity search," in *ICLR*, 2019.

[30] J. Zhang, F. Zhan, C. Theobalt, and S. Lu, "Regularized vector quantization for tokenized image synthesis," in *CVPR*, 2023, pp. 18 467–18 476.

[31] H. Fang, P. Xiong, L. Xu, and Y. Chen, "Clip2video: Mastering video-text retrieval via image clip," *arXiv preprint arXiv:2106.11097*, 2021.

[32] J. Xu, T. Mei, T. Yao, and Y. Rui, "Msr-vtt: A large video description dataset for bridging video and language," in *CVPR*, 2016, pp. 5288–5296.

[33] P. Jin, H. Li, Z. Cheng, J. Huang, Z. Wang, L. Yuan, C. Liu, and J. Chen, "Text-video retrieval with disentangled conceptualization and set-to-set alignment," in *IJCAI*, 2023, pp. 938–946.

[34] D. Chen and W. B. Dolan, "Collecting highly parallel data for paraphrase evaluation," in *ACL*, 2011, pp. 190–200.

[35] L. Anne Hendricks, O. Wang, E. Shechtman, J. Sivic, T. Darrell, and B. Russell, "Localizing moments in video with natural language," in *ICCV*, 2017, pp. 5803–5812.

[36] A. Rohrbach, M. Rohrbach, and B. Schiele, "The long-short story of movie description," in *PR*. Springer, 2015, pp. 209–221.

[37] V. Gabeur, C. Sun, K. Alahari, and C. Schmid, "Multi-modal transformer for video retrieval," in *ECCV*, 2020, pp. 214–229.

[38] F. Caba Heilbron, V. Escorcia, B. Ghanem, and J. Carlos Niebles, "Activitynet: A large-scale video benchmark for human activity understanding," in *CVPR*, 2015, pp. 961–970.

[39] D. P. Kingma and J. Ba, "Adam: A method for stochastic optimization," in *ICLR*, 2015.

[40] S. Zhao, L. Zhu, X. Wang, and Y. Yang, "Centerclip: Token clustering for efficient text-video retrieval," in *SIGIR*, 2022, pp. 970–981.

[41] Y. Liu, P. Xiong, L. Xu, S. Cao, and Q. Jin, "Ts2-net: Token shift and selection transformer for text-video retrieval," in *ECCV*. Springer, 2022, pp. 319–335.

[42] S.-V. Bogolin, I. Croitoru, H. Jin, Y. Liu, and S. Albanie, "Cross modal retrieval with querybank normalisation," in *CVPR*, 2022, pp. 5194–5205.